Calibrated fluorescence imaging of tissue *in vivo*

Jianan Y. Qu[a] and Jianwen Hua
Department of Electrical and Electronic Engineering, Hong Kong University of Science and Technology, Clear Water Bay, Kowloon, Hong Kong, People's Republic of China

(Received 31 January 2001; accepted for publication 25 April 2001)

A calibrated fluorescence imaging system utilizing a combination of fluorescence and cross-polarization imaging technology is described and applied to tissue examination *in vivo*. The results show that the inhomogeneity of fluorescence excitation and collection across the irregular surface of the examined tissue is calibrated to a great extent by taking the ratio of the raw fluorescence image to the cross-polarized reflection image. The effects of optical properties of tissue on the calibrated fluorescence signals are studies on simulated tissue phantoms systematically. Using the calibrated fluorescence imaging technology, we demonstrate that different tissue can be clearly separated endoscopically and *in vivo* based on the calibrated fluorescence signal. © *2001 American Institute of Physics.* [DOI: 10.1063/1.1379980]

Light-induced fluorescence (LIF) spectroscopy has been established as an effective technology in medical diagnosis with particular advantages for *in vivo* noninvasive characterization of pathological states in human tissue. It has been found that under the same excitation and collection geometry the fluorescence intensity of lesions is almost always lower than that of surrounding normal tissue.[1–3] This information could be used to detect the early lesions. Unfortunately, a common LIF imaging device for wide area surveillance of lesions cannot provide homogeneous illumination and fluorescence collection. To image lesions based on the contrast in LIF intensity between the lesion and the normal tissue, a calibration mechanism must be applied to correct the effects on LIF signal caused by the varying illumination/collection geometry across the imaged tissue surface.

Recently, we introduced a combined fluorescence and polarization imaging method that corrects the geometrical effect and creates a calibrated LIF image of tissue-like turbid media.[4] The mechanism of the correction for geometrical effects was investigated through a Monte Carlo modeling technique in an extended study.[5] It was shown that when both the fluorescence (F) and diffuse reflectance (R) are collected at a small angle from the incident axis of the illumination, the geometrical effects can be compensated by taking the F/R ratio. For a LIF endoscopic imaging system with a polarized excitation, the crossed source and detector arrangement can remove any specular reflection that does not carry information about illumination/collection geometry and extract the diffuse reflectance.[6,7] In this letter, we demonstrate the classification of tissue *in vivo* using a calibrated fluorescence endoscopic system based on the combined fluorescence and cross-polarization imaging technology.

A schematic of the calibrated fluorescence endoscopic system is shown in Fig. 1. A laser of wavelength at 457 nm is used as the excitation source. The endoscope is specially designed with a linear polarizer at the tip of the illumination channel as shown in Fig. 1. The diameters of the endoscope and the imaging lens are 7 and 3 mm, respectively. An optical fiber conducts the laser to the input port of the illumination channel. A dichroic mirror of cut-on wavelength of 470 nm divides the F and R signals collected by the endoscope into the fluorescence and reflection channels. The specular reflection is rejected by a polarizer (P) in the reflection channel with the polarization axis perpendicular to the illumination channel. The cross-polarized reflection image is recorded with a charge coupled device (CCD) camera. An additional bandpass filter (F) of a wavelength transmission range from 470 to 650 nm is used in the fluorescence channel to reject the residual excitation light. The raw fluorescence image is recorded with an ICCD camera. The video signals from the CCD and ICCD are captured by a frame grabber simultaneously at the rate of 25 frames per second. The F/R ratio image is generated by normalizing the fluorescence image to the cross-polarized reflection image and then multiplying it by a scaling constant.

To demonstrate the ability of the F/R ratio imaging technique for the correction of the geometrical effects *in vivo*, we imaged the oral and oropharyngeal tissues of an adult subject (one of the authors). The distance from the distal tip of the endoscope to the imaged tissue varied from 10 to 30 mm. The excitation power at the distal tip of the endoscope was

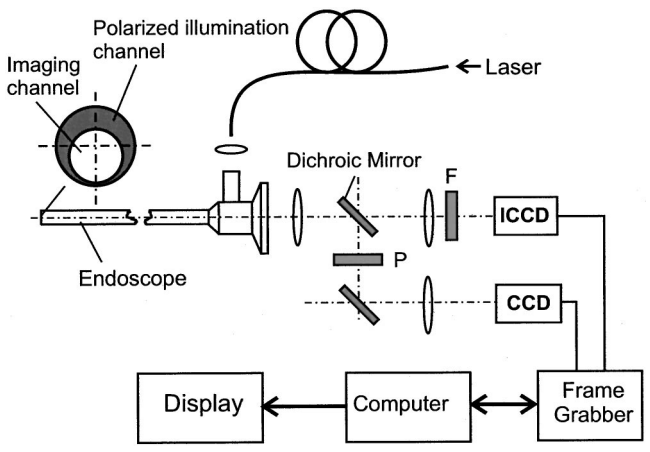

FIG. 1. A schematic of the F/R ratio endoscopic imaging system.

[a]Author to whom correspondence should be addressed; electronic mail: eequ@ust.hk

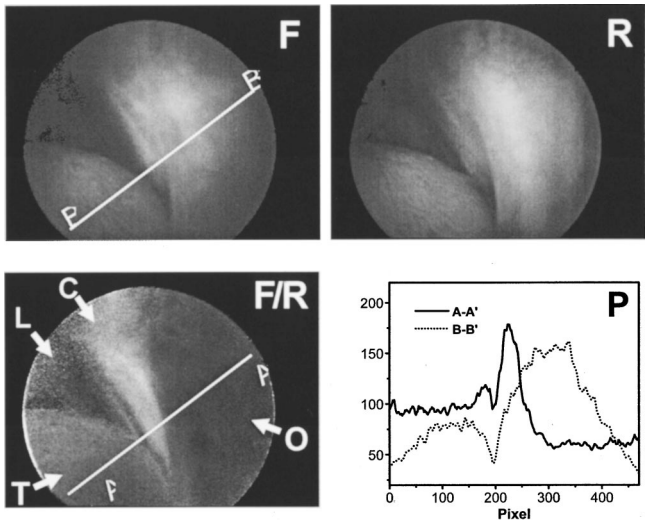

FIG. 2. Images recorded at the site of tongue, oral tissue, and connective tissue. Above: raw fluorescence image (F) and cross-polarized reflection image (R); Below: F/R ratio image (F/R) and line profiles across line $A-A'$ in F/R image and line $B-B'$ in F image (P).

kept about 20 mW to avoid saturating the ICCD. Figures 2 and 3 show the images obtained from the oral cavity and oropharynx sites. The F and R images in Fig. 2 were taken from the site where three kinds of tissues, tongue, oral tissue, and connective tissue between the oral cavity and oropharynx are presented in the field of view. As can be seen in image F of Fig. 2, the raw fluorescence signal varies in a wide range even within the same kind of tissue due to the geometrical effects. It is impossible to separate the tongue, oral tissue, and connective tissue based on the raw fluorescence intensity signal. However, the three different kinds of tissues are clearly separated in the F/R ratio image. The mean pixel values for tongue (indicated by arrow T in F/R ratio image), oral tissue (indicated by arrow O), and connective tissue (indicated by arrow C) are 93, 64, and 181, respectively. The F/R value from the same kind of tissue is uniform. The nonuniformity of fluorescence excitation and

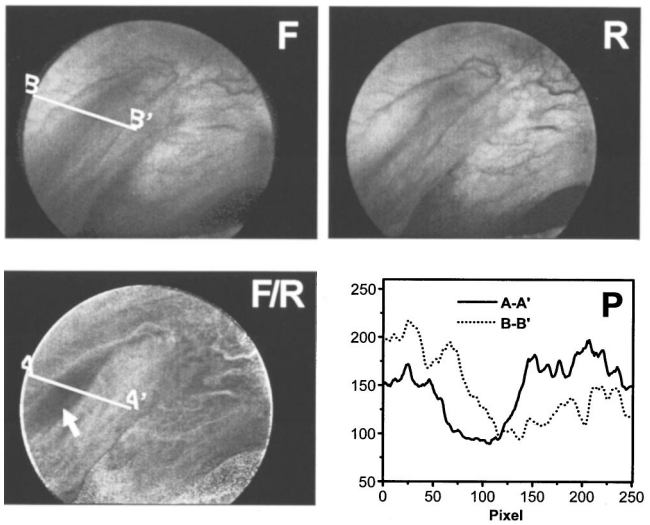

FIG. 3. Images recorded at the site of oropharynx. Above: raw fluorescence image (F) and cross-polarized reflection image (R); Below: F/R ratio image (F/R) and line profiles across line $A-A'$ in F/R image and line $B-B'$ in F image (P).

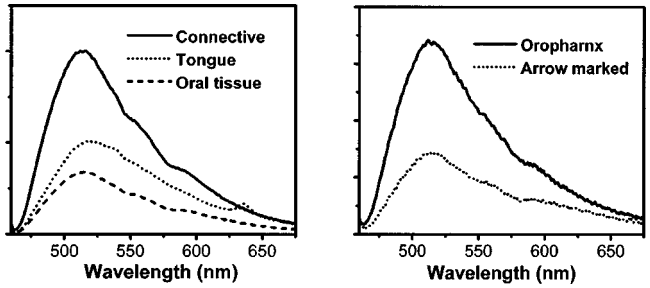

FIG. 4. Tissue fluorescence spectra measured with optical fiber catheter. Left: tongue, oral tissue, and connective tissue; Right: oropharyngeal tissue and tissue marked by the arrow in F/R image of Fig. 3.

collection are well calibrated. The area indicated by arrow L in the F/R image of Fig. 2 has fluorescence and reflection signal levels close to the dark charge backgrounds of ICCD and CCD. The F/R ratio value in the area is thus not reliable. The line profile analysis displayed in Fig. 2 provides a quantitative comparison before and after the calibration of LIF signals. Figure 3 displays the images recorded from an oropharynx site where many blood vessels are present. The raw fluorescence image again shows widely distributed pixel values. The calibrated F/R image demonstrates the good correction for the geometrical effects. In particular, a small area of relatively lower fluorescence (indicated by the arrow in F/R image of Fig. 3) can be clearly identified. The mean pixel values for the low fluorescence area and the surrounding tissue are 82 and 161, respectively. The line profiles in Fig. 3 present the quantitative difference between the small area of low fluorescence and surrounding oropharyngeal tissue.

To verify if the F/R ratio image provides a map of calibrated tissue fluorescence, we chose a well established optical fiber technique to measure the tissue fluorescence.[1–3] A multiple optic fiber catheter is used to deliver the 457 nm laser excitation and collect the fluorescence from the same tissue sites as shown in Figs. 2 and 3. The structure of the fiber catheter is the same as used in Ref. 3. During the measurement, the distal tip of the catheter is perpendicularly touched onto the tissue surface to ensure a fixed excitation and collection geometry at any tissue site. The measured fluorescence is then self-calibrated when the excitation is constant. The fluorescence is analyzed with a commercial spectrometer and the spectra are shown in Fig. 4. Each spectrum in Fig. 4 is an average of ten spectra recorded from ten different locations of the same kind of tissue. The difference of tissue fluorescence in tongue, oral tissue, connective tissue, and oropharyngeal tissue is obvious. To compare the results obtained from the measurements using an optic fiber catheter and F/R ratio imaging, we integrate the fluorescence spectral signal over the range from 470 to 650 nm, the same range as the bandpass filter in the fluorescence channel of the F/R endoscope device. The relative integrated fluorescence intensity in oral tissue, tongue, and connective tissue are $1\pm0.2{:}1.7\pm0.4{:}3.0\pm0.5$, compared with the relative F/R values at the same tissue sites of $1\pm0.1{:}1.5\pm0.2{:}2.9\pm0.3$. The relative fluorescence intensity in oropharyngeal tissue and the tissue site indicated by the arrow in the F/R image of Fig. 3 is $1\pm0.4{:}2.22\pm0.7$, compared with relative mean

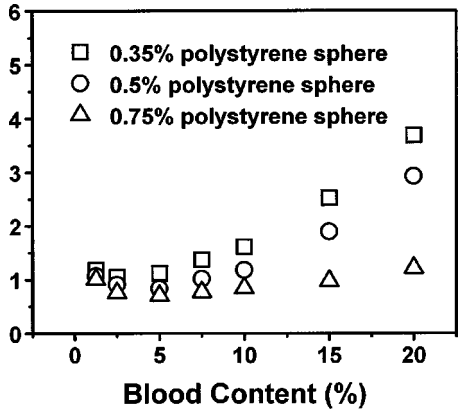

FIG. 5. Dependence of F/R value on the optical properties of tissue phantoms.

F/R values of 1 ± 0.2:1.96 ± 0.5. The results of F/R imaging are consistent with the fiber catheter measurements.

For living tissues with the same structure, the optical properties may not necessarily be homogeneous mainly because of variation in the local perfusion. We used the tissue-simulated phantoms to study how the optical properties of tissue affect the calibration of LIF signal in F/R ratio. A total of 21 tissue phantoms were made of fluorescent dye mixture as fluorophore, hemoglobin extracted from mice blood as dominant absorber, and polystyrene spheres of 0.55 μm in diameter as scattering agent in phosphate-buffered saline. The scattering properties of polystyrene microsphere, the LIF spectrum of dye mixture, and the procedure for extraction of hemoglobin were described in Ref. 5. The scattering coefficients of tissue phantoms spanned over the typical range of human tissue.[8,9] The blood contents in tissue phantoms were varied in wide range from 1% to 20%. The concentration of fluorescence dye in all the tissue phantoms were kept constant. We examined the tissue phantoms with the F/R ratio imaging system. The measured F/R values from all the phantoms are shown in Fig. 5. As can be seen, the F/R value is weakly dependent on the absorption when the blood content is not over 7.5%, which indicates that the effect of blood absorption on fluorescence and cross-polarized reflection may cancel to each other, and the small variation in the local perfusion may not significantly corrupt the correction for the geometrical correction and affect the fluorescence calibration. This is because the sampling depths

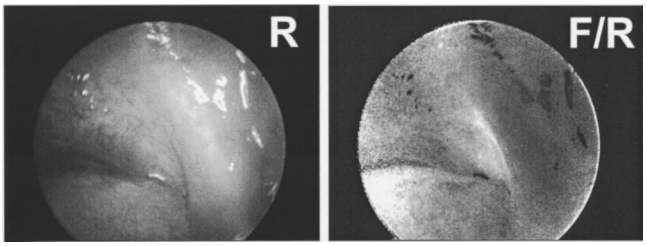

FIG. 6. Reflection and F/R ratio images recorded at the site of tongue, oral tissue, and connective tissue.

of both F and R images are the same and determined by the distribution of the excitation source in tissue. However, the F/R value increases quickly when the blood content is over 10%. This explains that the blood vessels in Fig. 3 always give higher F/R value than the surrounding tissue. It is found that F/R value is dependent on the scattering properties that are mainly determined by tissue structure. The variation of scattering properties over the imaged tissue surface may introduce artifacts for the correction of geometrical effects.

In the final experiment, we demonstrate the importance of the cross-polarization arrangement. We removed the polarizer in the reflection channel and allowed the specular reflection to be included in the R image. The F and R images were taken from the same tissue site as shown in Fig. 2. The reflection and F/R images are shown in Fig. 6. As can be seen, the specular reflection introduces significant artifacts in the F/R image and distorts the calibration.

The authors acknowledge the support from Hong Kong Research Grants Council under Grant No. HKUST6052/00M.

[1] R. M. Cothren, R. R. Richards-Kortum, M. V. Sivak, M. Fitzmaurice, R. P. Rava, G. A. Boyce, G. B. Hayes, M. Doxtader, R. Blackman, T. Ivanc, M. S. Feld, and R. E. Petras, Gastrointest. Endosc. **36**, 105 (1990).
[2] N. Ramanujam, M. F. Mitchell, A. Mahadevan, S. Thomsen, E. Silva, and R. Richards-Kortum, Gynecol. Oncology. **52**, 31 (1994).
[3] J. Qu, C. MacAulay, S. Lam, and B. Palcic, Opt. Eng. **34**, 3334 (1995).
[4] J. Y. Qu, Z. J. Huang, and J. W. Hua, Appl. Phys. Lett. **76**, 970 (2000).
[5] J. Y. Qu, Z. J. Huang, and J. W. Hua, Appl. Opt. **39**, 3344 (2000).
[6] S. G. Demos and R. R. Alfano, Appl. Opt. **36**, 150 (1997).
[7] S. L. Jacques, J. R. Roman, and K. Lee, Lasers Surg. Med. **26**, 119 (2000).
[8] W. F. Cheong, S. A. Prahl, and A. J. Welch, IEEE J. Quantum Electron. **26**, 2166 (1990).
[9] V. Tuchin, *Tissue Optics: Light Scattering Methods and Instruments for Medical Diagnosis* (SPIE-The International Society for Optical Engineering, Bellingham, WA, 2000).